environmental microbiology

Environmental Microbiology (2021) **00**(00), 00–00 doi:10.1111/1462-2920.15341

Analysis of bacterial communities in a municipal duck pond during a phytoplankton bloom and isolation of *Anatilimnocola aggregata* gen. nov., sp. nov., *Lacipirellula limnantheis* sp. nov. and *Urbifossiella limnaea* gen. nov., sp. nov. belonging to the phylum *Planctomycetes*

Nicolai Kallscheuer[1†] **Patrick Rast**,[2†] **Mareike Jogler**,[3] **Sandra Wiegand**,[1,4] **Timo Kohn**,[1] **Christian Boedeker**,[2] **Olga Jeske**,[2] **Anja Heuer**,[2] **Christian Quast**,[5] **Frank Oliver Glöckner**,[6] **Manfred Rohde**[7] **and Christian Jogler**[3*]

[1]*Department of Microbiology, Radboud University, Nijmegen, The Netherlands.*

[2]*Leibniz Institute DSMZ, Braunschweig, Germany.*

[3]*Department of Microbial Interactions, Institute of Microbiology, Friedrich Schiller University, Jena, Germany.*

[4]*Institute for Biological Interfaces 5, Karlsruhe Institute of Technology, Germany.*

[5]*Max Planck Institute for Marine Microbiology, Bremen, Germany.*

[6]*Alfred Wegener Institute, Helmholtz-Zentrum für Polar- und Meeresforschung, Bremerhaven, Germany.*

[7]*Central Facility for Microscopy, Helmholtz Centre for Infection Research, Braunschweig, Germany.*

Summary

Waterbodies such as lakes and ponds are fragile environments affected by human influences. Suitable conditions can result in massive growth of phototrophs, commonly referred to as phytoplankton blooms. Such events benefit heterotrophic bacteria able to use compounds secreted by phototrophs or their biomass as major nutrient source. One example of such bacteria are Planctomycetes, which are abundant on the surfaces of marine macroscopic phototrophs; however, less data are available on their ecological roles in limnic environments. In this study, we followed a cultivation-independent deep sequencing approach to study the bacterial community composition during a cyanobacterial bloom event in a municipal duck pond. In addition to cyanobacteria, which caused the bloom event, members of the phylum *Planctomycetes* were significantly enriched in the cyanobacteria-attached fraction compared to the free-living fraction. Separate datasets based on isolated DNA and RNA point towards considerable differences in the abundance and activity of planctomycetal families, indicating different activity peaks of these families during the cyanobacterial bloom. Motivated by the finding that the sampling location harbours untapped bacterial diversity, we included a complementary cultivation-dependent approach and isolated and characterized three novel limnic strains belonging to the phylum *Planctomycetes*.

Received 21 July, 2020; accepted 24 November, 2020. *For correspondence. E-mail christian.jogler@uni-jena.de; Tel. (+49) 3641 949301; Fax (+49) 3641 949302 †These authors contributed equally to this work.

Introduction

Aquatic primary biomass production is influenced by physical parameters, e.g. temperature, pH and light availability, and is coupled to availability of inorganic compounds (serving as sources of nitrogen or phosphate or as trace elements) (Duarte and Cebrián, 1996; Boulion, 2004). Given the ubiquitous nature of carbon dioxide (CO_2), the combination of above-mentioned parameters determines the overall rate of biomass production by phototrophic organisms in aquatic environments. Consequentially, aquatic habitats are typically categorized by the level of nutrients. Oceans are mostly oligotrophic (i.e. low nutrient levels) (Platt *et al*., 1983), whereas limnic environments are often eutrophic (i.e. higher levels of nutrients) (Blindow *et al*., 1993). Such differences have direct implications for growth of heterotrophic (micro)organisms as secondary producers,

which rely on biomass of primary producers as source of carbon and energy. Due to the smaller size of limnic environments (lakes, ponds, etc.), they are typically more sensitive to seasonal variation and the impact of human intervention is higher (Abrantes *et al*., 2006).

Under suitable conditions, availability of high levels of nutrients and minerals can result in excessive growth of phytoplankton, commonly referred to as algal blooms (Backer *et al*., 2015). Such events are caused by mass development of a limited number of species of algae or cyanobacteria accumulating directly at or below the water surface (Mohamed *et al*., 2003). Phytoplankton blooms can provide beneficial conditions for heterotrophic bacteria, which derive carbon and energy either from the algal biomass itself or by degrading compounds secreted by algae. One example of such bacteria are Planctomycetes, which were isolated from different abiotic and biotic surfaces in aquatic habitats (Bengtsson and Øvreås, 2010; Lage and Bondoso, 2014; Boersma *et al*., 2019; Kallscheuer *et al*., 2020). With relative abundances of up to 60%–85%, members of the phylum *Planctomycetes* were shown to be particularly frequent on surfaces of macroscopic phototrophs, such as kelp and seagrass, thus representing the dominant bacterial phylum in certain habitats (Wiegand *et al*., 2018; Kohn *et al*., 2020a). In this context, members of the class *Planctomycetia* within the phylum *Planctomycetes* were shown to perform a lifestyle switch, in which a sessile mother cell divides to yield a motile flagellated daughter cell, which in turn can attach to nearby surfaces by formation of a dedicated holdfast structure (Faria *et al*., 2018). The working hypothesis that Planctomycetes obtain carbon and energy from phototrophs is supported by the capability to degrade complex polysaccharides, e.g. the model compound dextran (Boedeker *et al*., 2017), as well as by the high number of putative carbohydrate-active enzymes encoded in their genomes (Naumoff, 2014; Kallscheuer *et al*., 2019b). A specialized morphology of several Planctomycetes, including fibres originating from conspicuous crateriform structures and an extremely enlarged cytoplasmic space, is probably functionally related to the uptake of entire polysaccharide molecules and their subsequent intracellular degradation (Boedeker *et al*., 2017). This strategy can provide a decisive advantage compared to the use of exoenzymes for the purpose of compound degradation. An exoenzyme-mediated degradation is associated with the risk that degradation products are flushed away or taken up by competing microorganisms occupying the same ecological niches as Planctomycetes.

Hitherto, it has been shown that Planctomycetes are frequently associated with micro- and macroalgae in marine habitats (Wiegand *et al*., 2018), while only a smaller number of strains has been isolated from freshwater bodies (Hirsch and Müller, 1985; Bondoso *et al*., 2011; Kohn *et al*., 2020b; Storesund *et al*., 2020). Consequentially, only little is known about their role in limnic environments.

In this study, we combined a cultivation-independent sequencing-based approach with targeted, cultivation-based methods to investigate bacterial community compositions during a phytoplankton bloom event in a duck pond in Wolfenbuettel, Lower Saxony, Germany. Using isolated DNA and RNA from two different sampling fractions as starting material (the attached- and the free-living fraction) allows to draw conclusions on the abundance and activity of different bacterial phyla. Based on the data obtained, we further analyzed the diversity in the phylum *Planctomycetes* on family and genus level and isolated and characterized three novel planctomycetal strains using a recently developed cultivation platform targeting members of this phylum.

Results and discussion

Two genera caused the cyanobacterial bloom event in the duck pond in Wolfenbuettel in 2012

During summer 2012, several cases of algal blooms were reported in Northern Germany, e.g., in the Binnenalster in Hamburg, in the rivers Havel and Spree close to Berlin and in the Greifswalder Bodden close to the island Ruegen in the Baltic Sea (information retrieved from local newspaper articles). We also observed a phytoplankton bloom in the duck pond in Wolfenbuettel in the same year and thus decided to analyze samples from this municipal pond. The duck pond (official name: Stadtgraben; engl. 'town moat') is located in the center of the town Wolfenbuettel, Lower Saxony, Germany (Fig. 1A), which has approximately 53 000 inhabitants. The pond itself has an area of approximately 20.000 m^2 (length: 450–550 m, width: 40–50 m), a maximal depth of 4.5 m and is inhabited by different fish and ducks. After processing of obtained samples, isolation of DNA and RNA and sequencing of the V3 region of 16S rRNA (gene) amplicons, we first analyzed data for the collected fractions (free-living fraction and attached fraction) on phylum level. Not surprisingly, with 58% relative abundance *Cyanobacteria* was the most abundant phylum in the attached fraction (particle size greater than 2.7 μm), however, only 1.1% of the sequences in the free-living fraction (size between 0.22 and 2.7 μm) could be traced back to this phylum (Fig. 1B). The phylum *Cyanobacteria* was also highly active in the attached fraction as confirmed by 98% relative abundance in the RNA samples (Fig. 1B). During a more detailed analysis of the sequences in the entire dataset, it turned out that 62% of the *Cyanobacteria*-derived sequences could be assigned to the genus *Snowella* and 27% to the genus *Microcystis*

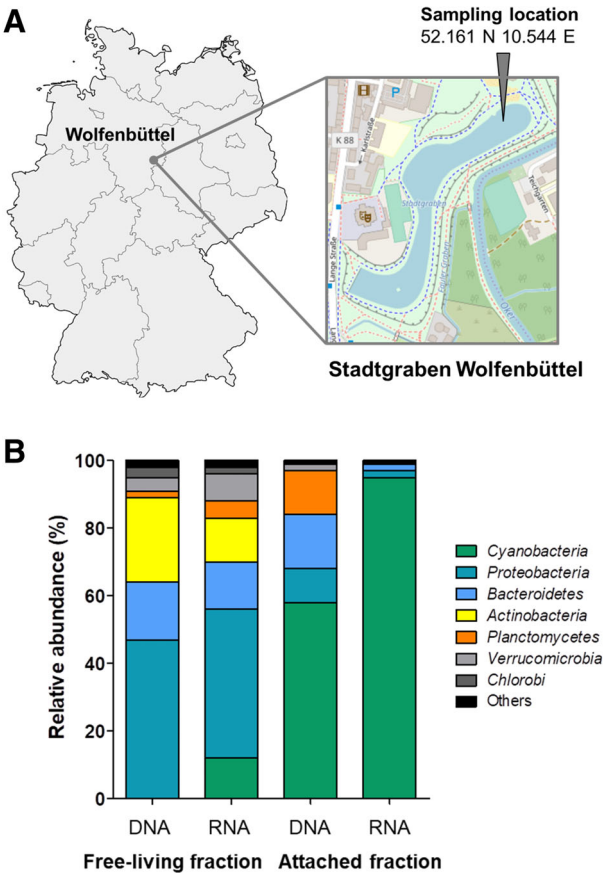

Fig 1. Sampling location (A) and results of the cultivation-independent bacterial community analysis on phylum level (B). The maps were obtained from OpenStreetMap. The cultivation-independent analysis is based on the following numbers of obtained sequences: 369 765 sequences (free-living fraction, DNA), 237 836 sequences (free-living fraction, RNA), 283 194 sequences (attached fraction, DNA) and 653 048 sequences (attached fraction, RNA).

(both family *Microcystaceae*). The residual 11% were assigned to 24 additional cyanobacterial families with individual abundances between 0.2% and 1.0%. Sequence analysis yielded a maximal similarity of 99.4% (a single mismatch in two of the obtained sequences over a length of 167 nucleotides) to *Snowella litoralis* strain 0TU37S04 (Rajaniemi-Wacklin *et al*., 2006) (GenBank acc. no. AJ781040). Members of the genus *Snowella* were shown to occur in freshwater or in slightly brackish biotopes, mainly in phytoplankton of large slightly eutrophic reservoirs (Guiry *et al*., 2014). While occurrence of several species was suggested to be restricted to limited areas, two species, *S. litoralis* and *Snowella lacustris*, possess worldwide distribution (Elenkin, 1938). The genus *Microcystis* contains species forming single cells or colonies, which occur in moderately eutrophic freshwater and are known to cause heavy water blooms (Lemmermann, 1910). During electron microscopic analysis of samples from the duck pond, *Snowella* and *Microcystis* morphotypes could be observed (Fig. 2), providing additional support that the phytoplankton bloom was primarily caused by members of these two genera. Cells of *S. litoralis* strain 0TU37S04 are spherical and have an average cell diameter of 3.1 μm (Rajaniemi-Wacklin *et al*., 2006). Characteristic aggregates observed during electron microscopy showed sizes of around 60 × 40 μm, which probably explains why cyanobacteria were mainly observed in the attached fraction.

Cultivation-independent analysis of other bacterial phyla in the duck pond samples

Municipal shallow waters, such as the investigated duck pond, are fragile environments and subject to rapid shifts of environmental conditions (also due to human influences). The observed phytoplankton bloom is expected to lead to an excess of biomass in the pond, thereby attracting microorganisms capable of degrading compounds secreted by cyanobacteria or the cyanobacterial biomass itself. We were curious to investigate the abundance and activity of different non-cyanobacterial phyla in the samples and thus compared the attached fraction (dominated by cyanobacteria) to the free-living fraction using our cultivation-independent approach (Fig. 1B). In addition to cyanobacteria, *Bacteroidetes* (16%), *Planctomycetes* (13%) and *Proteobacteria* (10%) turned out to be abundant phyla in the attached fraction. *Bacteroidetes* and *Proteobacteria* also showed a high abundance in the free-living fraction (47% and 17%, respectively), while members of the phylum *Actinobacteria* were nearly exclusively found in this fraction (ranked second, 25%). Activities in the free-living fraction (RNA samples) correlated to a large extent with the respective abundance of the observed phyla (Fig. 1B).

Members of the phylum *Planctomycetes* accounted for 2% of the bacterial diversity in the free-living fraction. The observed difference for this phylum when comparing the numbers of 13% in the attached fraction and 2% in the free-living fraction) are probably related to the preference of its members to attach to diverse biotic surfaces. Planctomycetes were previously shown to reach maximal relative abundances of 60%–85% on surfaces of kelp forests on the Californian coast or on seagrass leaves in the Mediterranean Sea (Wiegand *et al*., 2018; Kohn *et al*., 2020a). The preference for attached growth is also reflected by the results of our study when taking into account that the phylum *Planctomycetes* was more than six-fold enriched in the attached fraction compared to the free-living fraction. While ranked third in the attached fraction (DNA sample), an abundance of only 0.4% in the RNA fraction suggests that attached planctomycetal strains are present, but hardly active. In contrast, planctomycetal strains were less abundant but more active in the free-living fraction (Fig. 1B).

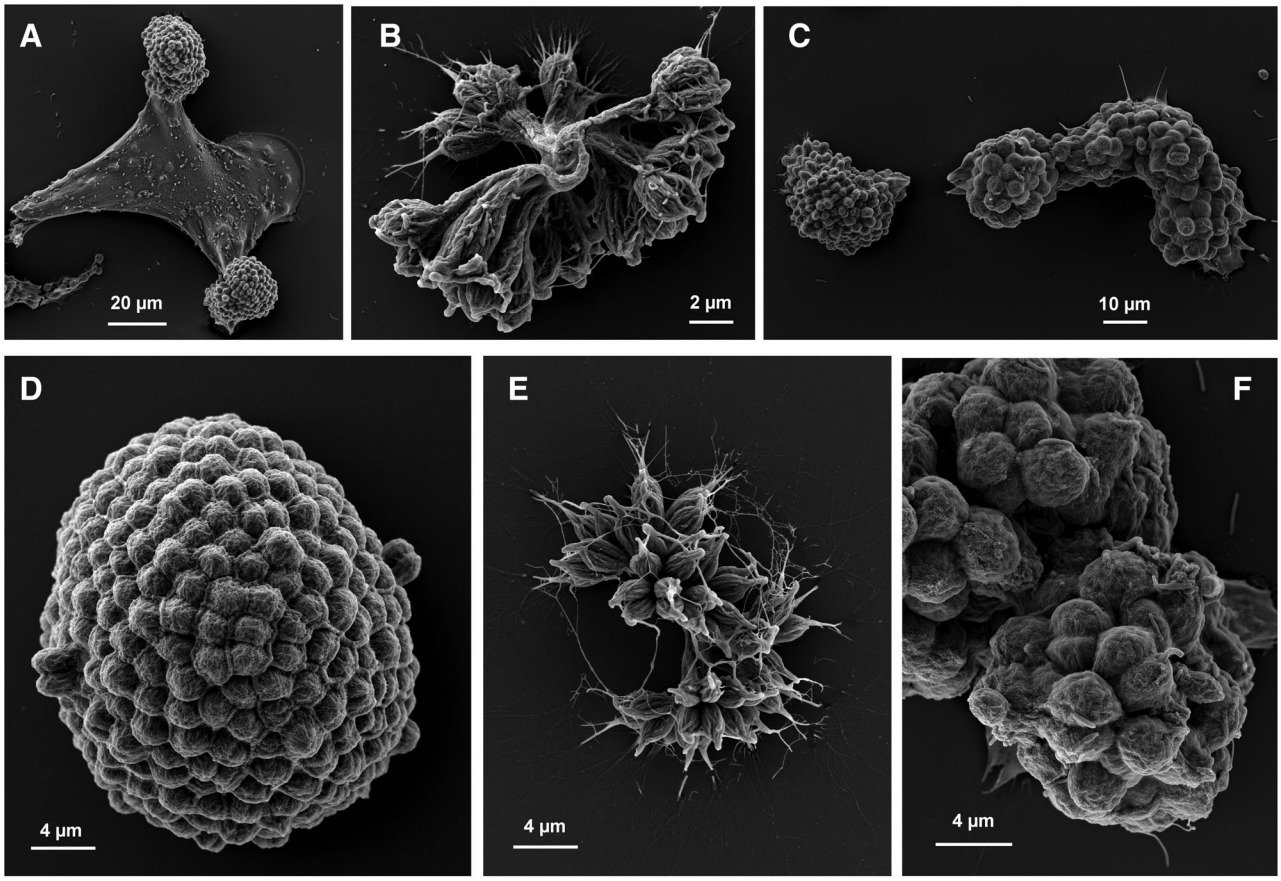

Fig 2. Scanning electron micrographs of *Snowella* and *Microcystis* morphotypes. The respective scale bars are indicated in each of the individual images.

In the attached fraction the phylum *Planctomycetes* showed a similar abundance level (DNA fraction) as the phylum *Bacteroidetes* (Fig. 1B). Among the abundant phyla obtained in this fraction *Bacteroidetes* is thereby also the most closely related phylum to *Planctomycetes* apart from *Verrucomicrobia* (Castelle and Banfield, 2018). Most sequences obtained for the phylum *Bacteroidetes* could be traced back to the family *Saprospiraceae* (order *Chitinophagales*), the env. OPS 17 clade (order *Sphingobacteriales*) and the genus *Fluviicola* (family *Crocinitomicaceae*, order *Flavobacteriales*). All three taxa are found in diverse aquatic habitats (including stagnant freshwater) and several described members were found to be involved in the breakdown of polymeric organic compounds in the environment, e.g. proteins (Xia *et al*., 2008), chitin and peptidoglycan (Eckert *et al*., 2013) or gelatin (O'Sullivan *et al*., 2005). A similar catabolic potential as observed for members of the phylum *Bacteroidetes* is also assumed for the phylum *Planctomycetes* and was already demonstrated for a small number of model strains earlier (Jeske *et al*., 2016). The coexistence of members of both phyla during the phytoplankton bloom is not unexpected and the assumption that genes coding for catabolic enzymes are exchanged by horizontal gene transfer is a plausible hypothesis to be addressed in future studies.

Analysis of planctomycetal operational taxonomic units on family and genus level

In our analysis using the SILVA database (reference version 132), a total number of 66 734 operational taxonomic units (OTUs) was obtained in the dataset, of which 3074 (4.6%) could be assigned to the phylum *Planctomycetes*, which is currently subdivided into the three classes *Planctomycetia*, *Phycisphaerae* and *Candidatus* Brocadiae. The class *Planctomycetia*, which currently contains the highest number of described species within the phylum, is further subdivided into the orders *Pirellulales*, *Planctomycetales*, *Gemmatales* and *Isosphaerales* with the respective families *Pirellulaceae*, *Planctomycetaceae*, *Gemmataceae*, and *Isosphaeraceae* (the order *Pirellulales* contains more than one family, however, the recently proposed families have not yet been implemented in the Silva-based taxonomy). On class level, around 80% of the identified *Planctomycetes*-OTUs fall within the class

Planctomycetia, 14% in the class *Phycisphaerae* and 0.1% in the class *Candidatus* Brocadiae. An analysis on family and genus level showed that 63% of the *Planctomycetes*-derived OTUs can be assigned to the family *Pirellulaceae* with the majority of sequences belonging to the genus *Rhodopirellula* (Fig. 3). Within the families *Gemmataceae* (11%), *Planctomycetaceae* (3%) and *Isosphaeraceae* (2%), around 90% of the obtained sequences belong to uncultivated genera, while the residual 10% could be assigned to described genera (Fig. 3). When taking into account that only around 140 strains of the phylum *Planctomycetes* have been characterized so far, high numbers of strains belonging to uncultivated genera are not unexpected. At the same time, the untapped planctomycetal diversity also underlines that the here investigated habitat is a valuable source for the isolation of hitherto uncharacterized species.

Comparison of abundance and activity of Planctomycetes in the attached fraction

The data obtained for the attached fraction yielded a relative abundance of 12.7% for members of the phylum *Planctomycetes* (isolated DNA, Fig. 1). However, isolated RNA of this fraction only led to 0.37% of the obtained sequences, which we could trace back to this phylum. Such numbers indicate that attached-living planctomycete strains are quite abundant during the phytoplankton bloom, but hardly active. We thus analyzed in more detail which families are abundant and which are among the active ones. Analysis of abundance values showed that the attached fraction was dominated by *Pirellulaceae* (89.0% of Planctomycete-derived sequences), whereas the families *Planctomycetaceae*, *Gemmataceae*, *Isosphaeraceae* and the class *Phycisphaerae* only represented minor fractions with relative abundances between 1.6% and 3.7% (Fig. 4). In the case that activities of planctomycetal strains present in the attached fraction correlate with their abundance, a similar distribution pattern should also be expected for sequence numbers obtained from isolated RNA. Evaluation of the activity data, however, led to a completely different picture. Nearly half of the planctomycete-derived sequences in the RNA samples (50.6%) could be assigned to the class *Phycisphaerae* (Fig. 4). Despite high abundance of the family *Pirellulaceae*, only every 10th sequence of planctomycetal origin could be traced back to this family in the dataset obtained from isolated RNA. For the other families,

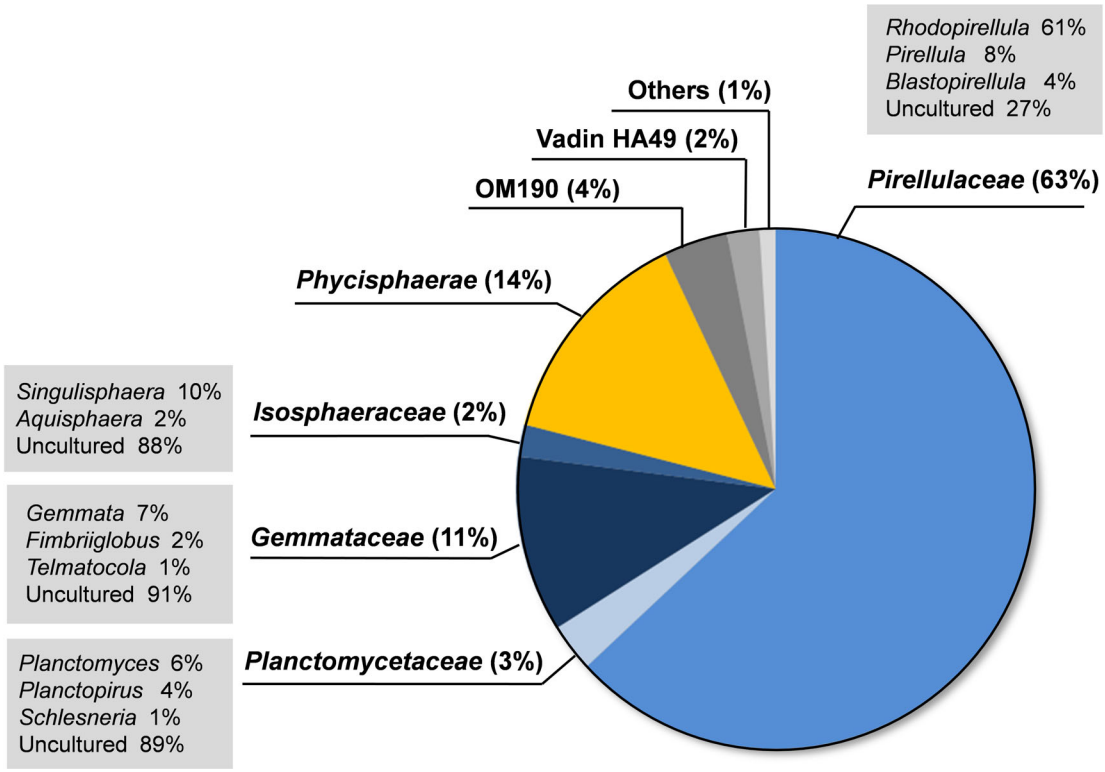

Fig 3. Analysis of obtained operational taxonomic units (OTUs) of the phylum *Planctomycetes* in the entire dataset. The percentages shown for the classes and families are based on the total number of planctomycete OTUs of 3074 (=100%). Percentages shown in the grey boxes refer to the OTUs of the individual families (=100%). Families belonging to different orders in the class *Planctomycetia* are shown in different shades of blue.

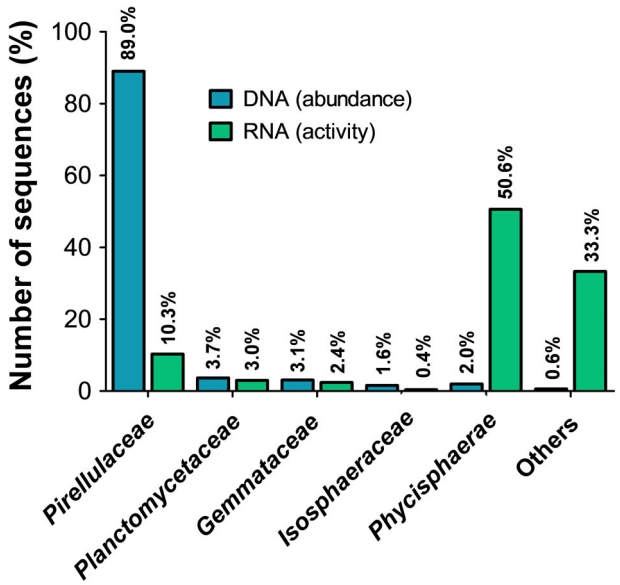

Fig 4. Analysis of abundance and activity of members of the phylum *Planctomycetes* in the attached fraction. The analysis is based on the obtained sequences assigned to the phylum *Planctomycetes*, distributed among the shown classes/families. The following numbers of sequences were obtained: 36 093 sequences (12.7% of all obtained sequences in the sample; isolated DNA), 2423 sequences (0.37% of all obtained sequences in the sample; cDNA from isolated RNA).

abundance and activity levels were comparable (Fig. 4). Strains of uncultured clades accounted for 33% of the sequences in the RNA samples originating from Planctomycetes (24% belonging to clade OM190 and 9% to clade vadin HA49).

The data suggest that *Pirellulaceae* is the most abundant planctomycetal family in the attached fraction, but hardly active, while members of the class *Phycisphaerae* are less abundant, but highly active. This might be explained by different lifestyles followed by strains belonging to the family *Pirellulaceae* and the class *Phycisphaerae*, a hypothesis that requires additional attention in future studies. A striking difference when comparing members of the two phylogenetically distinct groups is their genome size. Strains of the class *Phycisphaerae* characterized so far have rather small genomes of 3.1–4.3 Mb (Fukunaga *et al*., 2009; Pradel *et al*., 2020), whereas *Pirellulaceae* have considerably larger genomes of 6–10 Mb (Clum *et al*., 2009; Peeters *et al*., 2020). Planctomycetes are believed to degrade compounds released by (dying) phototrophs or the biomass itself, which then serve as nutrient source. For *Pirellulaceae*, this hypothesis is supported by the presence of large numbers of carbohydrate-active enzymes (Gade *et al*., 2005; Wegner *et al*., 2013), in turn requiring larger genomes. In contrast, smaller genomes of *Phycisphaerae* point towards smaller numbers of encoded catabolic enzymes and a less complex metabolism. Relatively high abundance, but low activity of the family *Pirellulaceae* may indicate that such strains are in a waiting position and only become active when cyanobacterial biomass starts to decay. High abundance or even dominance of *Pirellulaceae* during algal blooms is in line with previously published results (Morris *et al*., 2006; Cai *et al*., 2013). The recent discovery of the brominated aromatic compound 3,5-dibromo-*p*-anisic acid produced by a Planctomycete and potentially acting as algicide points towards a metabolic link between Planctomycetes and phototrophs (Panter *et al*., 2019). Despite the smaller genomes and a suggested lower versatility for degradation of algal compounds, *Phycisphaerae* strains were also isolated from algal surfaces (Fukunaga *et al*., 2009; Yoon *et al*., 2014). Low abundance and high activity of *Phycisphaerae* at the time point of sampling thus might indicate that different classes in the phylum *Planctomycetes* benefit from phytoplankton blooms at different life stages of the phototroph. Analysis of shifts in the bacterial community composition and clarification of our working hypothesis, however, requires a time-resolved study based on samples taken at different stages of phytoplankton blooms. Despite the 'snapshot' character of the here presented study, the dataset is a promising starting point for future studies.

Characterization of three novel Planctomycetes isolated from the duck pond

Based on the high number of sequences from uncultivated Planctomycete strains in the dataset, we considered the chosen sampling location an attractive source for the isolation and characterization of novel planctomycetal species. Hence, we also included a cultivation-dependent approach complementary to the cultivation-independent analysis and describe the characterization of three novel strains designated ETA_A1^T, ETA_A8^T and I41^T, which could be assigned to the phylum *Planctomycetes* after initial sequencing of the 16S rRNA gene. For the three isolates, we analyzed their phylogenetic positions in more detail and investigated morphological, physiological and genomic chracteristics.

Phylogenetically, the novel strains belong to three different families. In phylogenetic trees based on 16S rRNA gene sequences and multilocus sequence analysis (MLSA), strain ETA_A1^T clusters with members of the familiy *Gemmataceae*, strain ETA_A8^T within the family *Pirellulaceae* and strain I41^T within the recently introduced family *Lacipirellulaceae* (Fig. 5 and Supporting Information Fig. S1). Strain ETA_A1^T shows a 16S rRNA gene sequence similarity of <90.4% to characterized members of the family *Gemmataceae*, which is below the proposed genus threshold of 94.5% and suggests delineation of the strain from known genera in this family

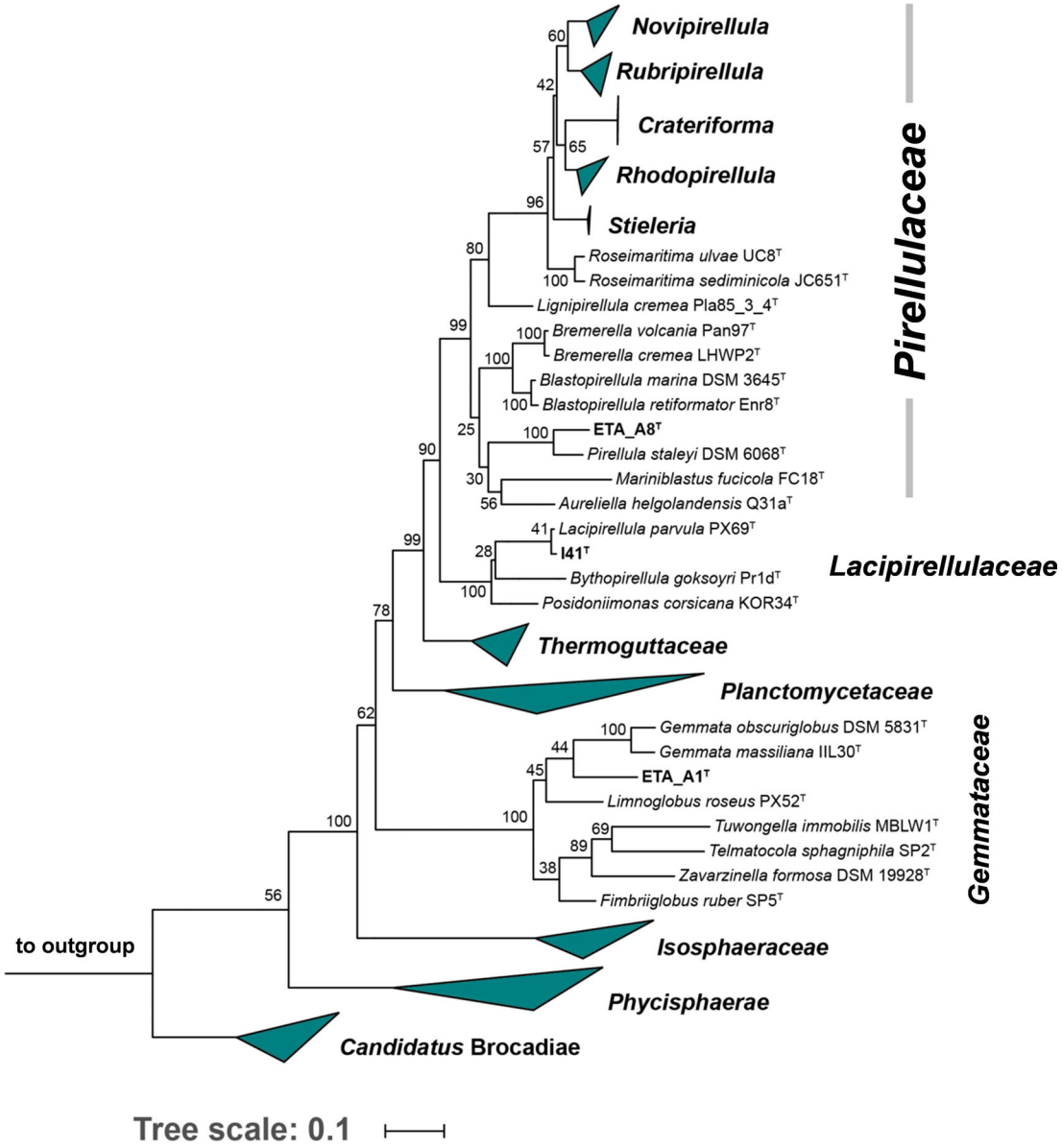

Fig 5. Maximum likelihood phylogenetic tree based on 16S rRNA gene sequences. Methodologies used for tree assembly are provided in the Experimental procedures sections. Bootstrap values obtained after 1000 resamplings are shown at each node in %. Three strains from the *Planctomycetes-Verrucomicrobia-Chlamydiae* (PVC) superphylum outside of the phylum *Planctomycetes* served as outgroup.

(Supporting Information Fig. S2). A maximal average nucleotide identity (ANI) of 73.3% obtained during comparison of strain ETA_A1^T with strains belonging to the genus *Gemmata* and type strains of other genera ensures that the strain is not a member of a characterized species (species threshold 95%, Supporting Information Fig. S2) (Kim *et al*., 2014). To consolidate the results suggested by 16S rRNA gene sequence similarity and ANI, we took additional phylogenetic markers into account. Comparison of strain ETA_A1^T with characterized members of the genus *Gemmata* yielded minimal average amino acid identity (AAI) values of 62.8% and percentage of conserved proteins (POCP) values of 56.8%. While the AAI is within the genus threshold range of 60%–80% (Konstantinidis and Tiedje, 2005), POCP is slightly above the genus threshold of 50% (Qin *et al*., 2014). Taken together, two out of three markers support delineation from the genus *Gemmata* and all other known genera in the family *Gemmataceae* (Supporting Information Fig. S2). Hence, we propose to assign the strain to a novel genus within this family.

The second isolate, strain ETA_A8^T, is a member of the family *Pirellulaceae* (Fig. 5 and Supporting Information Fig. S1) and all phylogenetic markers suggest

Pirellula staleyi as its current closest relative (Supporting Information Fig. S3). While similarity of the 16S rRNA gene sequence (93.7%) and AAI (59.4%) are below the respective genus threshold, POCP (55.3%) is slightly above the proposed threshold. For the family *Pirellulaceae*, a 1200 bp partial sequence of the gene *rpoB* coding for the β-subunit of RNA polymerase is also applicable as phylogenetic marker (Bondoso *et al*., 2013). Comparison of the partial *rpoB* sequence of strain ETA_A8^T with *P. staleyi* yielded a similarity of 83.6%, which is above the proposed genus threshold range of 75.5%–78% (Kallscheuer *et al*., 2019b). Two out of four phylogenetic markers support delineation of strain ETA_A8^T from the genus *Pirellula* and one could argument both in favour and against placing the novel strain in a novel genus. However, assignment of strain ETA_A8^T to the genus *Pirellula* would imply to disregard the genus threshold for 16S rRNA gene sequence similarity, although it has proven to be highly reliable in previous studies. Thus, we concluded to delineate strain ETA_A8^T from the genus *Pirellula* and all other described genera in the family *Pirellulaceae* and propose to place it in a novel genus.

Our third isolate, strain I41^T, clusters with the recently described species *Lacipirellula parvula* in both phylogenetic trees (Dedysh *et al*., 2019a) (Fig. 5 and Supporting Information Fig. S1). Analysis of phylogenetic markers is in line with delineation of the novel strain from the species *L. parvula*, but not from the genus *Lacipirellula*. Although the 16S rRNA gene sequence similarity of 99.1% obtained during comparison of strain I41^T with *L. parvula* PX69^T is slightly above the proposed species threshold of 98.7% (Stackebrandt and Ebers, 2006), an ANI of 78.1% and AAI of 78.4% far below the species threshold of 95% (Kim *et al*., 2014) clearly support delineation of the novel isolate from the species *L. parvula* (Supporting Information Fig. S4).

Next, we also analyzed basic morphological, physiological and genomic features of the three novel isolates (Figs. 6 and 7, Supporting Information Fig. S5) and used this data for a comparison of strains ETA_A1^T, ETA_A8^T and I41^T with the current closest relatives, namely *G. obscuriglobus*, *P. staleyi* and *L. parvula*, respectively (Table 1). Strain ETA_A1^T showed significant similarities to *G. obscuriglobus*, e.g. with regard to cell size and division, temperature optimum and range (pH range and optimum have not been analyzed for *G. obscuriglobus*) and colony pigmentation. Both, strain ETA_A1^T and *G. obscuriglobus*, display conspicuous crateriform structures and fimbriae, but lack a stalk and a holdfast structure. Under optimal conditions during laboratory-scale cultivation in M1H NAG medium, strain ETA_A1^T showed a maximal growth rate of 0.021 h^{-1}, which corresponds to a generation time of 33 h. Differences to *G. obscuriglobus* were mainly found during comparison of the genomes. With a size of 9.0 Mb, the genome of *G. obscuriglobus* is 15% larger than that of strain ETA_A1^T, whereas the G + C content of *G. obscuriglobus* is slightly lower (67.4% vs. 71.3%). Between 43% and 48% of the putative protein-coding genes in the two genomes are of unknown function.

More pronounced morphological differences were observed during comparison of strain ETA_A8^T with *P. staleyi*. Cells of strain ETA_A8^T are slightly larger and have a more elongated cell shape. While *P. staleyi* harbours a holdfast-structure and crateriform structures at one of the cell poles, these structures were not observed in case of strain ETA_A8^T. Both strains form white colonies. Optimal growth of strain ETA_A8^T (μ_{max} = 0.034 h^{-1}, generation time of 20 h) was observed at 30°C and pH 8.0, while no data was available for *P. staleyi*. Comparison on genome level revealed a highly similar G + C content of 57%–58%, but a considerable difference in the genome size. Strain ETA_A8^T (genome size of 9.0 Mb) harbours a much larger genome than *P. staleyi* (6.2 Mb). However, the relative number of putative proteins with unknown function is higher in *P. staleyi* (55%) than in strain ETA_A8^T(45%).

The current closest relative of strain I41^T is the recently described facultative anaerobic *L. parvula* PX69^T isolated from a boreal lake (Dedysh *et al*., 2019a). Our phylogenetic analysis suggests that strain I41^T is a novel species within the recently described genus *Lacipirellula*, thus significant similarities between the two strains are not unexpected, e.g. in the case of cell size, morphology and colony pigmentation. However, *L. parvula* harbours crateriform structures and a holdfast structure, which we could not observe for strain I41^T. Instead, strain I41^T produces a dense network of matrix or fimbriae. The strain reached a maximal growth rate of 0.016 h^{-1} and thus generation times of 43 h in M1H NAG medium. On the genome level, we observed a highly similar genome size and G + C content of 6.8–6.9 Mb and 61%–62%, respectively. In strain I41^T, the genomic information is distributed among a chromosome of 6 777 282 bp and a 53.7 kb plasmid. Astonishingly, 66% of the overall number of proteins encoded by *L. parvula* are of unknown function, a considerably higher number compared to typical numbers of 40%–55% observed in Planctomycetes including strain I41^T (47%).

Taken together, based on the phylogenetic analysis and supported by differences in morphological, physiological or genomic features, we conclude that the three strains ETA_A1^T, ETA_A8^T and I41^T represent three novel species belonging to two novel genera and the chracterized genus *Lacipirellula*. The genus and species protologues are provided below. We propose the names *Urbifossiella limnaea* gen. nov, sp. nov., *Anatilimnocola*

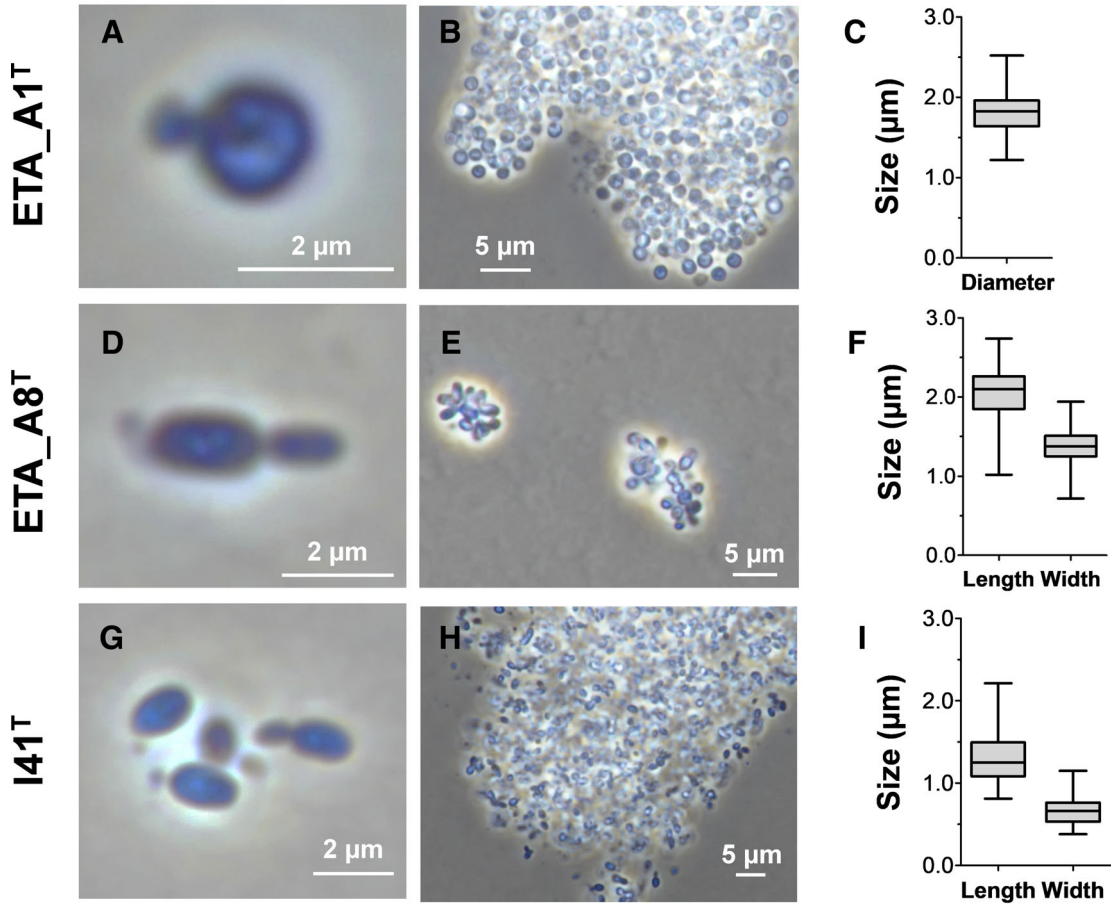

Fig 6. Light microscopic photographs and cell size plots of the isolates. The cell sizes were determined by manually measuring at least 100 cells or by applying a semi-automated object count tool. The scale bar is indicated in each of the individual pictures.

aggregata gen. nov., sp. nov. and *Lacipirellula limnantheis* sp. nov. for the strains ETA_A1^T, ETA_A8^T and I41^T, respectively. All three strains belong to the class *Planctomycetia*, which is in line with the observed abundance of members of this class during analysis of the planctomycete-derived sequences in the cultivation-independent approach. We also checked for presence of the 16S rRNA gene sequences of the three novel isolates in the dataset. In case of strain ETA_A8^T, we found the exact sequence of the V3 region, whereas a minimum of three and four mismatches in the V3 regions was observed for strain ETA_A1^T and I41^T, respectively.

Description of Urbifossiella *gen. nov.*

Ur.bi.fos.si.el'la. L. fem. n. *urbs* a town, city; L. fem. *n. fossa* a moat, ditch; N.L. fem. n. *Urbifossiella* a bacterium isolated from a town moat.

Cells have a cell envelope architecture resembling that of Gram-negative bacteria, are spherical, occur as single cells or in larger aggregates and reproduce by budding. The entire cell surface is covered with crateriform structures, but cells lack a stalk or holdfast structure. Cells are heterotrophic, aerobic, mesophilic and neutrophilic. Pink to red colonies are formed. The genus belongs to the family *Gemmataceae*, order *Gemmatales*, class *Planctomycetia*, phylum *Planctomycetes*. The type species is *Urbifossiella limnaea*.

Description of Urbifossiella limnaea *sp. nov.*

lim.nae'a. N.L. fem. adj. *limnaea* (from Gr. fem. adj. *limnaia*) living in limnic waters; corresponding to the origin of the strain from limnic waters.

In addition to the genus characteristics cells have a size of 1.8 $\pm$ 0.2 µm, are round grain rice-shaped and form matrix or fibre covering the entire cell surface. Cells of the species are able to grow over a temperature range of 15–30°C with optimal growth at 24°C and at pH 5.5–9.0 (optimum at pH 7.5). The G + C content is 71%. The type

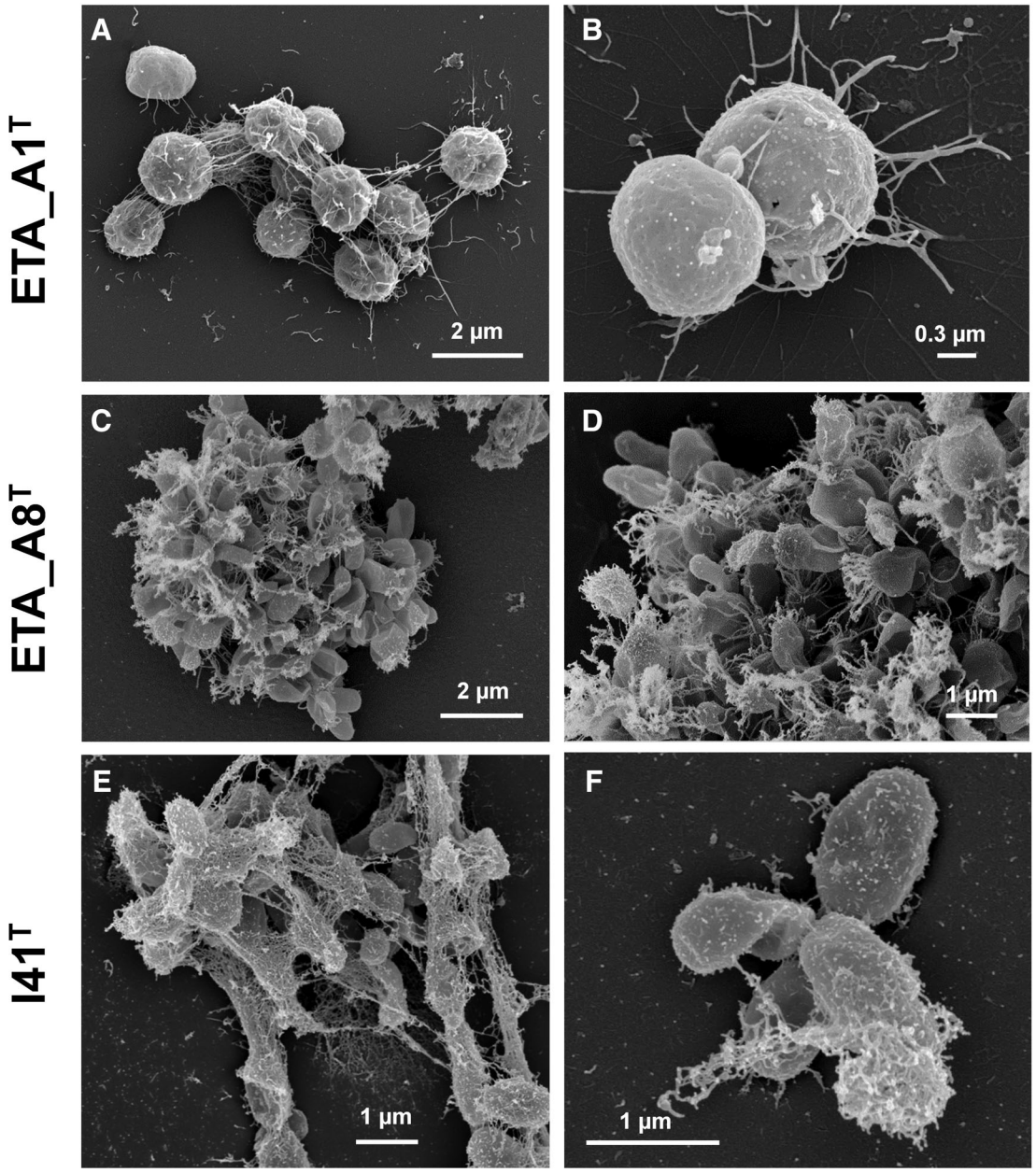

Fig 7. Electron micrographs of the novel isolates. Separate scale bars are indicated in each of the individual pictures.

strain is ETA_A1^T (= DSM 103724^T = LMG 29796^T) and was isolated during an algal bloom in a duck pond in Wolfenbuettel, Germany in April 2014.

Description of Anatilimnocola *gen. nov.*

A.na.ti.lim.no'co.la. L. fem. n. *anas*, duck; Gr. fem. n. *limne*, water, ditch; L. suff. *cola*, an inhabitant, dweller; N.L. fem. n. *Anatilimnocola* an inhabitant of a duck pond.

Cells with a Gram-negative cell envelope. Have an elongated shape, occur as rosettes, single cells or in larger aggregates and reproduce by polar budding. Crateriform structures, stalk and holdfast structure are not observed. Cells are heterotrophic, aerobic and mesophilic. White colonies are formed. The genus belongs to the family *Pirellulaceae*, order *Pirellulales*, class *Planctomycetia*, phylum *Planctomycetes*. The type species is *Anatilimnocola aggregata*.

Description of Anatilimnocola aggregata *sp. nov.*

ag.gre.ga'ta. N.L. fem. adj. *aggregata* aggregated; corresponding to the characteristic of the cells to form aggregates.

Table 1. Comparison of phenotypic and genomic features of the novel isolates and their current closest relatives. The genome analysis is based on GenBank accession numbers for the novel isolates given in the Experimental procedures section and acc. no. CP042911 (*Gemmata obscuriglobus*), CP001848 (*Pirellula staleyi*) and AP021861 (*Lacipirellula parvula*). 'Giant genes' refers to genes >15 kb. Abbreviations: n.o. not observed, n.d. not determined.

Strain	ETA_A1^T	*Gemmata obscuriglobus*	ETA_A8^T	*Pirellula staleyi*	I41^T	*Lacipirellula parvula*
Phenotypic features						
Length × width (μm)	1.8 ± 0.2 (diameter)	1.4–3.0	2.0 ± 0.3 × 1.4 ± 0.2	1.0–1.5 × 0.9–1.0	1.3 ± 0.3 × 0.7 ± 0.1	0.9–1.4 × 0.5–0.9
Shape	Spherical	Spherical to pear shaped	Round grain rice shaped	Drop to pear shaped	Pear shaped	Ellipsoidal
Colony colour	Pink to red	Rose	White	White	White	White
Temperature range (optimum) (°C)	15–30 (24)	16–35 (24)	15–33 (30)	n.d.	22–33 (30)	10–30 (20–25)
pH range (optimum)	5.5–9.0 (7.5)	n.d.	5.0–10.0 (8.0)	n.d.	5.0–9.0 (7.0)	5.0–7.5 (6.5)
Aggregates	Yes	Yes	Yes	Yes	Yes	Yes
Division mode	Budding	Budding	Budding	Budding	Budding	Budding
Dimorphic life cycle	n.o.	Yes	Yes	n.d.	n.o.	Yes
Relation to oxygen	Aerobic	Aerobic	Aerobic	Strictly aerobic	Aerobic	Facultatively anaerobic
Flagella	n.o.	Yes	n.o.	Yes	n.o.	Yes
Crateriform structures	Overall	Yes	n.o.	Yes, at one pole	n.o.	Yes, polar
Fimbriae	Overall matrix or fibre	Yes	Overall matrix or fibre	n.d.	Matrix or fibre	n.d.
Stalk	n.o.	No	n.o.	No	n.o.	No
Holdfast structure	n.o.	No	n.o.	Yes	n.o.	Yes
Genomic features						
Genome size (bp)	7 795 793	8 999 201	9 007 740	6 196 199	6 830 976	6 922 258
Plasmids	No	No	No	No	1	No
G + C content (%)	71.3	67.4	57.8	57.5	62.0 ± 3.0	61.7
Completeness (%)	94.83	94.83	100	98.28	96.55	96.55
Contamination (%)	5.17	6.03	5.17	0	3.45	3.45
Total genes	6369	7600	7134	4767	5623	5665
Genes per Mb	817	845	792	769	823	818
Protein-coding genes	6237	7465	7033	4705	5526	5581
Hypothetical proteins	2705	3608	3178	2601	2604	3702
Protein-coding genes per Mb	800	830	781	759	807	806
Coding density (%)	89.7	84.2	88.0	86.2	83.5	84.6
Giant genes	2	1	2	1	0	1
tRNAs	97	98	76	49	85	73
16S rRNA genes	2	5	1	1	1	1

In addition to the genus characteristics, cells have a size of 2.0 ± 0.3 × 1.4 ± 0.2 μm, form an extracellular matrix or fimbriae, and show optimal growth at 30°C and pH 8.0. Growth over a range of 15–33°C and pH 5.0–10.0 was observed. The genome has a G + C content of 57.8%. The type strain is ETA_A8^T (= LMG 29142^T= *STH00947*^{T}; the STH number refers to the Jena Microbial Resource Collection JMRC) and was isolated during an algal bloom in a duck pond in Wolfenbuettel, Germany in April 2014.

Description of Lacipirellula limnantheis *sp. nov.*

limn.an'the.is. Gr. fem. n. *limne* a lake, pond; Gr. neut. n. *anthos*, *antheos*, a flower, blossom; N.L. gen. n. *limnantheis* of a lake bloom.

Cells are pear-shaped with a size of 1.3 ± 0.3 × 0.7 ± 0.1 μm. Crateriform structures, stalk and holdfast structure are not observed. Produce extracellular matrix or fimbriae. Cells are heterotrophic, aerobic, mesophilic and neutrophilic. Growth is observed at 22–33°C (optimum 30°C) and pH 5.0–9.0 (optimum 7.0). Colonies lack pigmentation. The type strain is I41^T (= DSM 100603 ^{T} = LMG 29127^T, synonyms: Isolat 41, isolat41) and was isolated during an algal bloom in a duck pond in Wolfenbuettel, Germany in August 2012.

Conclusion

In this study, we performed a differentiated analysis of the bacterial community composition in a municipal duck pond during a cyanobacterial bloom. Separate datasets were generated based on the cyanobacteria-associated attached fraction and the free-living fraction as well as by separate analysis of 16S rRNA (gene) sequences from isolated DNA (abundance) and RNA

(activity). Analysis of the data showed that Planctomycetes were six-fold enriched in the attached fraction, which is in line with their suspected lifestyle on surfaces of phototrophs. Although the attached fraction was dominated by members of the family *Pirellulaceae* (class *Planctomycetia*), these strains were barely active. Instead, *Phycisphaerae* only showed minor abundance but turned out to be the most active class within the phylum. A time-resolved analysis is required to investigate whether different classes of the phylum *Planctomycetes* indeed show activity at different stages of the cyanobacterial bloom. Although of speculative nature at this early stage, we nevertheless would like to include the following working hypothesis: Given that known members of the class *Planctomycetia* have larger genomes than members of the class *Phycisphaerae*, they might harbour larger numbers of catabolic enzymes required for the breakdown of complex polysaccharides, of which the biomass of the phototroph is composed. This would imply that such strains become active at a later stage, at which the cyanobacterial biomass starts to decay. In contrast, due to smaller genomes *Phycisphaerae* probably lack an extensive enzymatic machinery needed for breakdown of biomass of the phototroph and might instead be well-adapted to use compounds secreted by vital and metabolically active phototrophs. If such a scenario is true, the activity peaks of *Phycisphaerae* and the phototroph would fall together, while the activity peak of the 'talented' degraders of the biomass of phototophs is shifted to a later stage (death phase of the phototroph).

Experimental procedures

Sampling and differential filtration

Three 300 ml surface freshwater samples were taken in a 2 m radius in a duck pond (Stadtgraben Wolfenbuettel, Germany, 52.161 N 10.544 E) during a phytoplankton bloom event on 30 August 2012. The three samples were filtered through a single borosilicate glass microfiber filter (GF/D, 47 mm, Whatman), which retains particles greater than 2.7 μm, e.g. phytoplankton and attached-living microorganisms. Subsequently, the filtrate obtained from the first filtration step was filtered through a 0.22 μm pore diameter Isopore polycarbonate membrane filter (47 mm, Millipore Merck) to obtain the free-living bacterial fraction. Both filters were stored at −20°C until DNA and RNA extraction. Strain I41^T was isolated from an additional water sample taken from the duck pond on 30 August 2012, while strains ETA_A1^T and ETA_8^T were obtained from a second sampling on 4 April 2014.

DNA extraction from filters

Genomic DNA from borosilicate glass microfiber and polycarbonate filters was extracted using a modified method based on previously published protocols (Fuhrman *et al*., 1988; Marschall *et al*., 2010). First, the half of each filter was cut into pieces using sterile scalpels and transferred to a 15 ml reaction tube. In the next step, 3 ml STE buffer [10 mM Tris hydrochloride (pH 8.0), 1 mM EDTA, 100 mM NaCl] with 1% (w/v) sodium dodecyl sulfate (SDS) was added to each tube and samples were boiled for 10 min. During boiling, samples were vortexted every 2 min. Subsequently, the buffer was removed by pipetting and collected in a separate 15 ml reaction tube. The remaining filter sections were mixed with 1.5 ml TE buffer (10 mM Tris hydrochloride, pH 8.0 and 1 mM EDTA) and boiled again for 10 min. TE buffer was then removed by pipetting and pooled with the collected STE buffer. Filter sections were discarded and the collected buffer pools were mixed with 4 ml phenol:chloroform:isoamylalcohol (25:24:1, v/v/v) and samples were incubated for 5 min at room temperature with shaking. Tubes were then centrifuged for 20 min at 4000*g* and the upper phase was re-extracted with 4 ml of chloroform, followed by 5 min incubation at room temperature with shaking. Again, the aqueous phase was collected after centrifugation for 20 min at 4000*g* and DNA was precipitated with 0.6 volumes of isopropanol at −20°C overnight. The DNA was pelleted by centrifugation (4000*g*, 4°C, 30 min). DNA pellets were washed twice with 70% (v/v) ice-cold ethanol, dried and resuspended in 50 μl PCR-grade H_2O. DNA concentrations were determined using the Qubit dsDNA BR Assay Kit and a Qubit 2.0 Fluorometer (Life Technologies GmbH). A DNA concentration of 18 ng μl^{-1} (glass microfiber filter) and 11 ng μl^{-1} (polycarbonate membrane filter), each in a volume of 50 μl H_2O, was obtained.

RNA extraction and cDNA synthesis

Total RNA from the second half of the borosilicate glass microfiber and polycarbonate filters was extracted using a modified version of a previously published protocol (Eichler *et al*., 2008; Marschall *et al*., 2010). Filter strips were combined with 0.5 g sterile glass beads (0.5 mm diameter, BioSpec Products), 600 μl of extraction buffer [50 mM sodium acetate, 10 mM EDTA, 0.1% (v/v) diethyl pyrocarbonate (DEPC), pH 4.2; 1% (w/v) *N*-lauroylsarcosine; sodium salt was added after autoclaving] and 600 μl of acidic phenol (Roti-aqua-Phenol, Roth). Filter sections were disrupted by bead-beating with a FastPrep-24 Instrument (MP Biomedicals) at maximum speed for 1 min and immediately placed on ice. Tubes were then centrifuged at 15 000*g* for 30 min at 4°C. After

centrifugation, the aqueous phase was collected and 0.1 volumes of 3 M sodium acetate solution (pH 5.2) and 1 volume of chloroform were added. Samples were vortexed and centrifuged for 10 min at 15 000*g* and 4°C. Afterwards, the chloroform extraction was repeated and the aqueous phase was collected. RNA was precipitated with 1 volume of isopropanol at −20°C overnight and was pelleted by centrifugation at 15 000*g* for 30 min at 4°C. RNA pellets were washed twice with 70% (v/v) ethanol diluted with DEPC-treated distilled water, air-dried and resuspended in 50 µl DEPC-treated water. DNase I (Thermo Scientific) was used to remove contaminating DNA. Each reaction contained a maximum of 400 ng RNA, 2 µl 10x reaction buffer with $MgCl_2$, 2 µl DNase I (RNase-free) and was filled up to a total volume of 20 µl with DEPC-treated sterile water. Tubes were incubated at 37°C for 1 h followed by addition of 2 µl EDTA (RNase-free, Thermo Scientific) and further incubation at 65°C for 10 min. After digestion of DNA, RNA was pooled and purified using the RNeasy MinElute Cleanup Kit (Qiagen) following the manufacturer's recommendation. Determination of the total RNA concentration was performed using a NanoDrop-1000 Spectrophotometer (PeqLab). RNA concentrations of 141 ng μl^{-1} (glass microfiber filter) and 17 ng μl^{-1} (polycarbonate membrane filter) were obtained (each in a total volume of 14 µl). Purified RNA was stored at −80°C until cDNA synthesis. An amount of 70 ng of purified RNA derived from either the glass microfiber or the polycarbonate filters was used for cDNA synthesis with the GoScript Reverse Transcription System (Promega) according to the manufacturer's description with random hexamer primers and 3 mM $MgCl_2$. As a control, one assay for each RNA sample was prepared without reverse transcriptase to detect internal DNA contamination. A second control assay was prepared without template RNA to exclude external DNA contaminations in subsequent PCR reactions. After synthesis, cDNA from both types of filters was stored at −20°C until further analysis.

Whole genome amplification

In order to generate higher quantities of genomic DNA necessary for Illumina multiplex sequencing, whole genome amplification (WGA) was applied using gDNA extracted from glass microfiber and polycarbonate filters as templates. The Illustra GenomiPhi V2 DNA Amplification Kit (GE Healthcare) was employed. For each amplification reaction, 1 ng of extracted DNA was used and three independent reactions were pooled to reduce stochastic amplification bias. To remove remaining amplification reagents from previous WGA reactions, pooled samples (60 µl total volume), mixed with 0.1 volumes of 3 M sodium acetate (pH 5.2), were purified by precipitation with 2.5 volumes of ethanol (96%, p.a. quality). Samples were inverted gently and incubated for 5 min at −20°C to allow precipitation. DNA was pelleted by centrifugation at 15 000*g* for 30 min at 4°C and washed twice with 150 µl ice cold ethanol by centrifugation for 15 min at 15 000*g* and 4°C. Pellets were then dried for 15 min at room temperature and resuspended in PCR-grade H_2O. Dissolution of DNA was performed for 10 min at 50°C under continuous agitation. The concentration of DNA was measured with the Qubit Fluorometer (Life Technologies GmbH). DNA concentrations of 27 ng μl^{-1} (glass microfiber filter sample, in a volume of 30 µl H_2O) and 24 ng μl^{-1} (polycarbonate membrane filter, in a volume of 25 µl H_2O) were obtained after WGA.

Barcoded PCR of variable region V3 of 16S rRNA genes for Illumina deep sequencing

Amplification of the V3 variable region of the bacterial 16S ribosomal RNA gene for deep sequencing analysis was performed by a modified procedure based on previously published protocols (Bartram *et al*., 2011; Caporaso *et al*., 2011). For genomic DNA templates, a first PCR was performed using 5 pmol of the primers uni341F (5'-CCT ACG GGW GGC WGC AG-3') and uni515R (5'-CCG CGG CTG CTG GCA C-3'). Each 50 µl reaction contained 500 ng of WGA-amplified genomic DNA and 1 unit of Phusion High-Fidelity DNA polymerase (New England Biolabs) with the provided 1x Phusion GC-buffer and dNTPs. PCR conditions included an initial denaturation step at 94°C for 7 min, followed by 10 cycles of 94°C for 1 min, 63°C for 1 min and 72°C for 1 min. Final elongation was performed at 72°C for 7 min.

In a second PCR, modified primers were used (Table 2). The V3_F forward primer was used in all reactions, but unique barcoded reverse primers were used for different samples. For genomic DNA derived from the glass microfiber filters the reverse primer V3R_57 and for the polycarbonate filter primer V3R_58 was included. Each PCR contained 10 pmol of each primer and 10 µl PCR amplificate from the first PCR reaction. The PCR conditions were the same as stated above with two modifications: the annealing temperature was increased to 65°C and 15 cycles were used. Per sample, five PCR reactions were pooled and used in metaphor gel electrophoresis.

RNA samples were amplified immediately after cDNA synthesis using 10 pmol of each barcoded reverse primer V3R_59 (glass microfiber filters) or V3R_60 (polycarbonate filters) in combination with the forward primer V3_F. For the PCR, an initial denaturation at 94°C for 3 min was followed by 15 cycles of 94°C for 15 s, 59°C for 15 s and 72°C for 15 s. Final elongation was performed at 72°C for 7 min. Per sample, two PCR reactions were

Table 2. Primers used for barcoded Illumina Sequencing.

Primer name	Sequence (5'–3')
V3_F	aatgatacggcgaccaccgagatctacactctttccctacacgacgctcttccgatctCCTACGGGWGGCWGCAG
V3R_57	caagcagaagacggcatacgagat**AGTCAT**gtgactggagttcagacgtgtgctcttccgatctCCGCGGCTGCTGGCAC
V3R_58	caagcagaagacggcatacgagat**AGAAGT**gtgactggagttcagacgtgtgctcttccgatctCCGCGGCTGCTGGCAC
V3R_59	caagcagaagacggcatacgagat**CTTATG**gtgactggagttcagacgtgtgctcttccgatctCCGCGGCTGCTGGCAC
V3R_60	caagcagaagacggcatacgagat**CTAGAA**gtgactggagttcagacgtgtgctcttccgatctCCGCGGCTGCTGGCAC

Lowercase letters denote adapter sequences necessary for binding to the flow cell, underlined lowercase letters are binding sites for the Illumina sequencing primers, bold uppercase letters highlight the index sequences and regular uppercase letters correspond to the V3 region primers uni 341F and uni 515R.

amplified and pooled. PCR amplicons were run on a metaphor agarose gel and cleaned up by gel extraction as described below.

Gel electrophoresis and purification of barcoded PCR products for Illumina deep sequencing

Analytical gels for Illumina multiplex sequencing templates were prepared at a concentration of 2% (w/v) high-resolution agarose (MetaPhor agarose, Lonza), adequate for the separation of small PCR products from resulting primer dimers. Gels were run in TAE buffer at 120 V for 150 min at 4°C and stained with SYBR Gold nucleic acid gel stain (Life Technologies) following the manufacturer's recommendations. DNA was visualized on a UV transilluminator equipped with a blue-light converter plate (Intas). DNA fragments of the desired band size were precisely excised using a clean scalpel and were extracted with the NucleoSpin Gel and PCR Clean-up kit (Macherey-Nagel). The 100 µl purified V3 amplicon of each filter, containing ~20 ng μl^{-1} amplicon each, were used for Illumina multiplex deep sequencing.

Illumina deep sequencing

V3 amplicon sequencing data (100 bp paired-end reads) obtained from Illumina multiplex sequencing (Miseq Analyser) was further processed. Raw sequencing data files were decompressed and raw sequences were trimmed to a value of 100 bp. Sequencing data were pre-processed by eliminating primer dimers, using the DimerFilter.jar script, based on a FASTQC-Adapter detection algorithm derived from the FASTQC program (Andrews, 2010). Subsequently, forward and reverse reads were joined using the program Fastq-join (Aronesty, 2013). All data were checked for chimeric sequences using the program Uchime (Edgar *et al*., 2011). The results for the dataset generated in this study are shown in Table 3.

Analysis using the SILVAngs analysis pipeline

Analysis of the multifasta files obtained after the chimera-check was performed using the web-based SILVAngs (Quast *et al*., 2013) analysis pipeline. Files were uploaded as suggested in the SILVAngs user-guide and data were processed by the SILVAngs software according to the protocol, including aligment with the SINA aligner (Pruesse *et al*., 2012). During the process, a de-replication step, eliminating 100% identical reads by only processing the longest read, as well as operational taxonomic unit (OTU) definition and clustering was performed (Li and Godzik, 2006). OTUs were classified by a local BLAST search using BLASTn version 2.2.3.0+ with default parameters in accordance with the non-redundant version of the SILVA SSU database, reference version 132. Classification of defined OTUs was visualized using the implemented software tool Krona (Ondov *et al*., 2011). For the entire dataset, the SILVAngs analysis yielded 66 734 unique sequences (14 sequences rejected), which cover a length between 105 and 194 bp with an average length of 176 bp. The sequences led to 63 094 OTUs (94.55%), 3353 clustered sequences (5.02%) and 273 replicates (0.41%). A number of 65 237 (97.76%) corresponds to classified sequences, for the other 1483 (2.22%) no relative could be identified.

Isolation of novel planctomycetal strains and cultivation

For the isolation of strains ETA_A1^T and ETA_A8^T M1H NAG medium with artificial freshwater (AFW) was prepared as described (Wiegand et al., 2020). About 20 µl of homogenized surface freshwater from the duck pond in Wolfenbuettel was plated on M1H NAG AFW plates supplemented with 8 g l^{-1} gellan gum, 200 mg l^{-1} ampicillin, 100 mg l^{-1} carbenicillin and 20 mg l^{-1} cycloheximide, which were then incubated at 18°C for 6 weeks. For the isolation of strain I41^T, M1H NAG medium without AFW was used and the plates were supplemented with 2000 mg l^{-1} carbenicillin and 20 mg l^{-1} cycloheximide. All strains were maintained in liquid M1H NAG medium. In order to verify that obtained strains are members of

Table 3. Key aspects of V3 amplicon samples derived from glass microfiber and polycarbonate filters, representing particle-associated or free-living bacteria, respectively.

Sample	Raw reads	Reads without primer dimers	Joined reads	Reads after chimera check
gDNA, glass microfiber filter	352 275	342 950	288 578	283 194
gDNA, polycarbonate filter	498 110	479 263	401 647	369 765
RNA, glass microfiber filter	791 028	788 278	659 445	653 048
RNA, polycarbonate filter	280 676	278 273	249 953	237 836
Total number of reads	1 922 089	1 888 764	1 599 623	1 543 843

Data were preprocessed employing the V3 amplicon data pipeline protocol (Bunk and Kaul, DSMZ, Brunswick).

the phylum *Planctomycetes*, the 16S rRNA gene was amplified by colony-PCR and sequenced as previously described (Rast *et al*., 2017).

Determination of pH and temperature optimum

Cultivations for determination of the pH optimum were performed in M1H NAG medium. A buffer concentration of 100 mM 4-(2-hydroxyethyl)-1-piperazineethanesulfonic acid (HEPES) was used for cultivations at pH 7–8. For cultivation at pH 5–6, HEPES was replaced by 100 mM 2-(*N*-morpholino)ethanesulfonic acid (MES), whereas 100 mM *N*-cyclohexyl-2-aminoethanesulfonic acid (CHES) served as a buffering agent at pH 9–10. Cultivations for determination of the pH optimum were performed at 28°C. Cultivations for determination of the temperature optimum were performed in standard M1H NAG medium at pH 7.5. Growth was analyzed by measuring optical densities at 600 nm (OD_{600}). For the calculation of growth rates, the natural logarithm of average OD_{600} values from biological triplicates was plotted against the cultivation time. The slope of the linear range of the plot (at least five data points) was used as maximal growth rate μ_{max}.

Microscopy protocols

Phase contrast and field emission scanning electron microscopy were performed as previously described (Boersma *et al*., 2019).

Genome information

The genome sequences of the novel strains ETA_A1^T and ETA_A8^T are available from GenBank under accession numbers CP036273 and CP036274, respectively. Sequence information for strain I41^T can be found under accession numbers CP036339 (chromosome) and CP036340 (plasmid pI41_1). The 16S rRNA gene sequences are available under accession numbers MK559972 (ETA_A1^T), MK559973 (ETA_A8^T) and MK554526 (I41^T). Genome sequencing is part of a previously published study (Wiegand *et al*., 2020). Gene prediction, protein annotation and determination of numbers of hypothetical or uncharacterized proteins were performed with Prokka v.1.11.

Phylogenetic analysis

The 16S rRNA gene sequence-based phylogeny was computed for the novel isolates, the type strains of all described planctomycetal species (assessed in May 2020) and all isolates recently published and described (Boersma *et al*., 2019; Dedysh *et al*., 2019b; Dedysh *et al*., 2019a; Kallscheuer *et al*., 2019a; Kallscheuer *et al*., 2019b; Kohn *et al*., 2020b; Kallscheuer *et al*., 2020; Rensink *et al*., 2020). The 16S rRNA gene sequences were aligned with SINA (Pruesse *et al*., 2012) and the phylogenetic inference was calculated with RAxML (Stamatakis, 2014) with a maximum likelihood approach with 1000 bootstraps, nucleotide substitution model GTR, gamma distributed rate variation and estimation of proportion of invariable sites (GTRGAMMAI option). For the multilocus sequence analysis (MLSA), the unique single-copy core genome of the analyzed genomes was determined with proteinortho5 (Lechner *et al*., 2011) with the 'selfblast' option enabled. The protein sequences of the resulting orthologous groups were aligned using MUSCLE v.3.8.31 (Edgar, 2004). After clipping, partially aligned *C*- and *N*-terminal regions and poorly aligned internal regions were filtered using Gblocks (Castresana, 2000). The final alignment was concatenated and clustered using FastTree (Price *et al*., 2009). The average nucleotide identity (ANI) was calculated using OrthoANI (Lee *et al*., 2016). The average amino acid identity (AAI) was calculated using the aai.rb script of the enveomics collection (Rodriguez-R and Konstantinidis, 2016) and the percentage of conserved proteins (POCP) was calculated as described (Qin *et al*., 2014). The *rpoB* nucleotide sequences were taken from publicly available planctomycetal genome annotations and the sequence identities were determined as described (Bondoso *et al*., 2013). Alignment and matrix calculation were performed with Clustal Omega (Sievers *et al*., 2011).

Acknowledgements

Part of this research was funded by the Deutsche Forschungsgemeinschaft grants KA 4967/1-1 and JO 893/4-1. The authors thank Ina Schleicher for skillful technical assistance. We also thank Brian Tindall and Regine Fähnrich from the DSMZ as well as the staff from the BCCM/LMG strain collection in Belgium and the Jena Microbial Resource Collection for support during strain deposition.

References

Abrantes, N., Antunes, S., Pereira, M., and Gonçalves, F. (2006) Seasonal succession of cladocerans and phytoplankton and their interactions in a shallow eutrophic Lake (Lake Vela, Portugal). *Acta Oecol* **29**: 54–64.

Andrews, S. (2010) *FastQC: A Quality Control Tool for High Throughput Sequence Data*. Cambridge, United Kingdom: Babraham Bioinformatics, Babraham Institute.

Aronesty, E. (2013) Comparison of sequencing utility programs. *Open Bioinforma J* **7**: 1–8.

Backer, L.C., Manassaram-Baptiste, D., LePrell, R., and Bolton, B. (2015) Cyanobacteria and algae blooms: review of health and environmental data from the harmful algal bloom-related illness surveillance system (HABISS) 2007–2011. *Toxins* **7**: 1048–1064.

Bartram, A.K., Lynch, M.D., Stearns, J.C., Moreno-Hagelsieb, G., and Neufeld, J.D. (2011) Generation of multimillion-sequence 16S rRNA gene libraries from complex microbial communities by assembling paired-end Illumina reads. *Appl Environ Microbiol* **77**: 3846–3852.

Bengtsson, M.M., and Øvreås, L. (2010) Planctomycetes dominate biofilms on surfaces of the kelp *Laminaria hyperborea*. *BMC Microbiol* **10**: 261.

Blindow, I., Andersson, G., Hargeby, A., and Johansson, S. (1993) Long-term pattern of alternative stable states in two shallow eutrophic lakes. *Freshwat Biol* **30**: 159–167.

Boedeker, C., Schuler, M., Reintjes, G., Jeske, O., van Teeseling, M.C., Jogler, M., *et al*. (2017) Determining the bacterial cell biology of Planctomycetes. *Nat Commun* **8**: 14853.

Boersma, A.S., Kallscheuer, N., Wiegand, S., Rast, P., Peeters, S.H., Mesman, R.J., *et al*. (2019) *Alienimonas californiensis* gen. nov. sp. nov., a novel Planctomycete isolated from the kelp forest in Monterey Bay. *Antonie Van Leeuwenhoek* **113**: 1751–1766. https://doi.org/10.1007/s10482-019-01367-4.

Bondoso, J., Harder, J., and Lage, O.M. (2013) *rpoB* gene as a novel molecular marker to infer phylogeny in *Planctomycetales*. *Antonie Van Leeuwenhoek* **104**: 477–488.

Bondoso, J., Albuquerque, L., Nobre, M.F., Lobo-da-Cunha, A., da Costa, M.S., and Lage, O.M. (2011) *Aquisphaera giovannonii* gen. nov., sp. nov., a planctomycete isolated from a freshwater aquarium. *Int J Syst Evol Microbiol* **61**: 2844–2850.

Boulion, V. (2004) Contribution of major groups of autotrophic organisms to primary production of water bodies. *Water Resour* **31**: 92–102.

Cai, H.-Y., Yan, Z.-S., Wang, A.-J., Krumholz, L.R., and Jiang, H.-L. (2013) Analysis of the attached microbial community on mucilaginous cyanobacterial aggregates in the eutrophic Lake Taihu reveals the importance of Planctomycetes. *Microb Ecol* **66**: 73–83.

Caporaso, J.G., Lauber, C.L., Walters, W.A., Berg-Lyons, D., Lozupone, C.A., Turnbaugh, P.J., *et al*. (2011) Global patterns of 16S rRNA diversity at a depth of millions of sequences per sample. *Proc Natl Acad Sci U S A* **108**: 4516–4522.

Castelle, C.J., and Banfield, J.F. (2018) Major new microbial groups expand diversity and alter our understanding of the tree of life. *Cell* **172**: 1181–1197.

Castresana, J. (2000) Selection of conserved blocks from multiple alignments for their use in phylogenetic analysis. *Mol Biol Evol* **17**: 540–552.

Clum, A., Tindall, B.J., Sikorski, J., Ivanova, N., Mavrommatis, K., Lucas, S., *et al*. (2009) Complete genome sequence of *Pirellula staleyi* type strain (ATCC 27377^{T}). *Stand Gen Sci* **1**: 308–316.

Dedysh, S.N., Kulichevskaya, I.S., Beletsky, A.V., Ivanova, A.A., Rijpstra, W.I.C., Damsté, J.S.S., *et al*. (2019a) *Lacipirellula parvula* gen. nov., sp. nov., representing a lineage of planctomycetes widespread in low-oxygen habitats, description of the family *Lacipirellulaceae* fam. nov. and proposal of the orders *Pirellulales* ord. nov., *Gemmatales* ord. nov. and *Isosphaerales* ord. nov. *Syst Appl Microbiol* **43**: 126050.

Dedysh, S.N., Henke, P., Ivanova, A.A., Kulichevskaya, I.S., Philippov, D.A., Meier-Kolthoff, J.P., *et al*. (2019b) 100-year-old enigma solved: identification, genomic characterization and biogeography of the yet uncultured *Planctomyces bekefii*. *Environ Microbiol* **22**: 198–211.

Duarte, C.M., and Cebrián, J. (1996) The fate of marine autotrophic production. *Limnol Oceanogr* **41**: 1758–1766.

Eckert, E.M., Baumgartner, M., Huber, I.M., and Pernthaler, J. (2013) Grazing resistant freshwater bacteria profit from chitin and cell-wall-derived organic carbon. *Environ Microbiol* **15**: 2019–2030.

Edgar, R.C. (2004) MUSCLE: multiple sequence alignment with high accuracy and high throughput. *Nucleic Acids Res* **32**: 1792–1797.

Edgar, R.C., Haas, B.J., Clemente, J.C., Quince, C., and Knight, R. (2011) UCHIME improves sensitivity and speed of chimera detection. *Bioinformatics* **27**: 2194–2200.

Eichler, S., Weinbauer, M.G., Dominik, K., and Höfle, M.G. (2008) Extraction of total RNA and DNA from bacterioplankton. In *Molecular Microbial Ecology Manual*, Kowalchuk, G.A., de Bruijn, F.J., Head, I.M., Akkermans, A.D., and van Elsas, J.D. (eds). Dordrecht, Netherlands: Springer, pp. 103–120.

Elenkin, A. (1938) Monographia algarum cyanophycearum aquidulcium et terrestrium in finibus URSS inventarum. *Sinezelenje vodorosli SSSR* **1**: 1–1908.

Faria, M., Bordin, N., Kizina, J., Harder, J., Devos, D., and Lage, O.M. (2018) Planctomycetes attached to algal surfaces: insight into their genomes. *Genomics* **110**: 231–238.

Fuhrman, J.A., Comeau, D.E., Hagström, Å., and Chan, A. M. (1988) Extraction from natural planktonic microorganisms of DNA suitable for molecular biological studies. *Appl Environ Microbiol* **54**: 1426–1429.

Fukunaga, Y., Kurahashi, M., Sakiyama, Y., Ohuchi, M., Yokota, A., and Harayama, S. (2009) *Phycisphaera*

mikurensis gen. nov., sp. nov., isolated from a marine alga, and proposal of *Phycisphaeraceae* fam. nov., *Phycisphaerales* ord. nov. and *Phycisphaerae* classis nov. in the phylum *Planctomycetes*. *J Gen Appl Microbiol* **55**: 267–275.

Gade, D., Gobom, J., and Rabus, R. (2005) Proteomic analysis of carbohydrate catabolism and regulation in the marine bacterium *Rhodopirellula baltica*. *Proteomics* **5**: 3672–3683.

Guiry, M.D., Guiry, G.M., Morrison, L., Rindi, F., Miranda, S. V., Mathieson, A.C., *et al*. (2014) AlgaeBase: an on-line resource for algae. Cryptogamie. *Algologie* **35**: 105–115.

Hirsch, P., and Müller, M. (1985) *Planctomyces limnophilus* sp. nov., a stalked and budding bacterium from freshwater. *Syst Appl Microbiol* **6**: 276–280.

Jeske, O., Surup, F., Ketteniß, M., Rast, P., Förster, B., Jogler, M., *et al*. (2016) Developing techniques for the utilization of Planctomycetes as producers of bioactive molecules. *Front Microbiol* **7**: 1242.

Kallscheuer, N., Jogler, M., Wiegand, S., Peeters, S.H., Heuer, A., Boedeker, C., *et al*. (2019a) Three novel *Rubripirellula* species isolated from plastic particles submerged in the Baltic Sea and the estuary of the river Warnow in northern Germany. *Antonie Van Leeuwenhoek* **113**: 1767–1778. https://doi.org/10.1007/s10482-019-01368-3.

Kallscheuer, N., Wiegand, S., Peeters, S.H., Jogler, M., Boedeker, C., Heuer, A., *et al*. (2019b) Description of three bacterial strains belonging to the new genus Novipirellula gen. nov., reclassificiation of *Rhodopirellula rosea* and *Rhodopirellula caenicola* and readjustment of the genus threshold of the phylogenetic marker *rpoB* for *Planctomycetaceae*. *Antonie Van Leeuwenhoek* **113**: 1779–1795. https://doi.org/10.1007/s10482-019-01374-5.

Kallscheuer, N., Wiegand, S., Heuer, A., Rensink, S., Boersma, A.S., Jogler, M., *et al*. (2020) *Blastopirellula retiformator* sp. nov. isolated from the shallow-sea hydrothermal vent system close to Panarea Island. In *Antonie Van Leeuwenhoek*, Vol. **113**, pp. 1811–1822. https://doi.org/10.1007/s10482-019-01377-2.

Kim, M., Oh, H.-S., Park, S.-C., and Chun, J. (2014) Towards a taxonomic coherence between average nucleotide identity and 16S rRNA gene sequence similarity for species demarcation of prokaryotes. *Int J Syst Evol Microbiol* **64**: 346–351.

Kohn, T., Rast, P., Wiegand, S., Jetten, M., Kallscheuer, N., Jeske, O., *et al*. (2020a) The microbiome of *Posidonia oceanica* seagrass leaves can be dominated by Planctomycetes. *Front Microbiol* **11**: 1458.

Kohn, T., Wiegand, S., Boedeker, C., Rast, P., Heuer, A., Schüler, M., *et al*. (2020b) *Planctopirus ephydatiae*, a novel Planctomycete isolated from a freshwater sponge. *Syst Appl Microbiol* **43**: 126022.

Konstantinidis, K.T., and Tiedje, J.M. (2005) Towards a genome-based taxonomy for prokaryotes. *J Bacteriol* **187**: 6258–6264.

Lage, O.M., and Bondoso, J. (2014) Planctomycetes and macroalgae, a striking association. *Front Microbiol* **5**: 267.

Lechner, M., Findeiss, S., Steiner, L., Marz, M., Stadler, P. F., and Prohaska, S.J. (2011) Proteinortho: detection of (co-)orthologs in large-scale analysis. *BMC Bioinform* **12**: 124.

Lee, I., Ouk Kim, Y., Park, S.C., and Chun, J. (2016) OrthoANI: an improved algorithm and software for calculating average nucleotide identity. *Int J Syst Evol Microbiol* **66**: 1100–1103.

Lemmermann, E. (1910) *Algen I. (Schizophyceen, Flagellaten, Peridineen)*, Leipzig, Germany: Gebrüder Borntraeger, Ulan Press.

Li, W., and Godzik, A. (2006) Cd-hit: a fast program for clustering and comparing large sets of protein or nucleotide sequences. *Bioinformatics* **22**: 1658–1659.

Marschall, E., Jogler, M., Henßge, U., and Overmann, J. (2010) Large-scale distribution and activity patterns of an extremely low-light-adapted population of green sulfur bacteria in the Black Sea. *Environ Microbiol* **12**: 1348–1362.

Mohamed, Z.A., Carmichael, W.W., and Hussein, A.A. (2003) Estimation of microcystins in the freshwater fish *Oreochromis niloticus* in an Egyptian fish farm containing a *Microcystis* bloom. *Environ Toxicol* **18**: 137–141.

Morris, R., Longnecker, K., and Giovannoni, S. (2006) *Pirellula* and OM43 are among the dominant lineages identified in an Oregon coast diatom bloom. *Environ Microbiol* **8**: 1361–1370.

Naumoff, D. (2014) Bioinformatic analysis of endo β-xylanases from Planctomycetes. In Ninth International Conference on the Bioinformatics of Genome Regulation and Structure/Systems Biology, Novosibirsk, p. 112.

Ondov, B.D., Bergman, N.H., and Phillippy, A.M. (2011) Interactive metagenomic visualization in a web browser. *BMC Bioinformatics* **12**: 385.

O'Sullivan, L.A., Rinna, J., Humphreys, G., Weightman, A.J., and Fry, J.C. (2005) *Fluviicola taffensis* gen. nov., sp. nov., a novel freshwater bacterium of the family *Cryomorphaceae* in the phylum '*Bacteroidetes*'. *Int J Syst Evol Microbiol* **55**: 2189–2194.

Panter, F., Garcia, R., Thewes, A., Zaburannyi, N., Bunk, B., Overmann, J., *et al*. (2019) Production of a dibrominated aromatic secondary metabolite by a planctomycete implies complex interaction with a macroalgal host. *ACS Chem Biol* **14**: 2713–2719.

Peeters, S.H., Wiegand, S., Kallscheuer, N., Jogler, M., Heuer, A., Jetten, M.S., *et al*. (2020) *Lignipirellula cremea* gen. nov., sp. nov., a planctomycete isolated from wood particles in a brackish river estuary. *Antonie Van Leeuwenhoek* **113**: 1863–1875. https://doi.org/10.1007/s10482-020-01407-4.

Platt, T., Rao, D.S., and Irwin, B. (1983) Photosynthesis of picoplankton in the oligotrophic ocean. *Nature* **301**: 702–704.

Pradel, N., Fardeau, M.-L., Tindall, B.J., and Spring, S. (2020) *Anaerohalosphaera lusitana* gen. nov., sp. nov., and *Limihaloglobus sulfuriphilus* gen. nov., sp. nov., isolated from solar saltern sediments, and proposal of *Anaerohalosphaeraceae* fam. nov. within the order *Sedimentisphaerales*. *Int J Syst Evol Microbiol* **70**: 1321–1330.

Price, M.N., Dehal, P.S., and Arkin, A.P. (2009) FastTree: computing large minimum evolution trees with profiles instead of a distance matrix. *Mol Biol Evol* **26**: 1641–1650.

Pruesse, E., Peplies, J., and Glöckner, F.O. (2012) SINA: accurate high-throughput multiple sequence alignment of ribosomal RNA genes. *Bioinformatics* **28**: 1823–1829.

Qin, Q.-L., Xie, B.-B., Zhang, X.-Y., Chen, X.-L., Zhou, B.-C., Zhou, J., *et al*. (2014) A proposed genus boundary for the prokaryotes based on genomic insights. *J Bacteriol* **196**: 2210–2215.

Quast, C., Pruesse, E., Yilmaz, P., Gerken, J., Schweer, T. (2013). The SILVA ribosomal RNA gene database project: improved data processing and web-based tools. *Nucleic Acids Research* **41**: D590–D596. https://dx.doi.org/10.1093/nar/gks1219.

Rajaniemi-Wacklin, P., Rantala, A., Mugnai, M.A., Turicchia, S., Ventura, S., Komárková, J., *et al*. (2006) Correspondence between phylogeny and morphology of *Snowella* spp. and *Woronichinia naegeliana*, cyanobacteria commonly occurring in lakes. *J Phycol* **42**: 226–232.

Rast, P., Glockner, I., Boedeker, C., Jeske, O., Wiegand, S., Reinhardt, R., *et al*. (2017) Three novel species with peptidoglycan cell walls form the new genus *Lacunisphaera* gen. nov. in the family opitutaceae of the verrucomicrobial subdivision 4. *Front Microbiol* **8**: 202.

Rensink, S., Wiegand, S., Kallscheuer, N., Rast, P., Peeters, S.H., Heuer, A., *et al*. (2020) Description of the novel planctomycetal genus *Bremerella*, containing *Bremerella volcania* sp. nov., isolated from an active volcanic site, and reclassification of *Blastopirellula cremea* as *Bremerella cremea* comb. nov. *Antonie Van Leeuwenhoek* **113**, 1823–1837.

Rodriguez-R, L.M., and Konstantinidis, K.T. (2016) The enveomics collection: a toolbox for specialized analyses of microbial genomes and metagenomes. *PeerJ* **4**: e1900v1.

Sievers, F., Wilm, A., Dineen, D., Gibson, T.J., Karplus, K., Li, W., *et al*. (2011) Fast, scalable generation of high-quality protein multiple sequence alignments using Clustal omega. *Mol Syst Biol* **7**: 539.

Stackebrandt, E., and Ebers, J. (2006) Taxonomic parameters revisited: tarnished gold standards. *Microbiol Today* **06**: 152–155.

Stamatakis, A. (2014) RAxML version 8: a tool for phylogenetic analysis and post-analysis of large phylogenies. *Bioinformatics* **30**: 1312–1313.

Storesund, J.E., Lanzèn, A., Nordmann, E.L., Armo, H.R., Lage, O.M., and Øvreås, L. (2020) *Planctomycetes* as a vital constituent of the microbial communities inhabiting different layers of the meromictic Lake Sælenvannet (Norway). *Microorganisms* **8**: 1150.

Wegner, C.-E., Richter-Heitmann, T., Klindworth, A., Klockow, C., Richter, M., Achstetter, T., *et al*. (2013) Expression of sulfatases in *Rhodopirellula baltica* and the diversity of sulfatases in the genus *Rhodopirellula*. *Mar Genomics* **9**: 51–61.

Wiegand, S., Jogler, M., and Jogler, C. (2018) On the maverick planctomycetes. *FEMS Microbiol Rev* **42**: 739–760.

Wiegand, S., Jogler, M., Boedeker, C., Pinto, D., Vollmers, J., Rivas-Marín, E., *et al*. (2020) Cultivation and functional characterization of 79 Planctomycetes uncovers their unique biology. *Nat Microbiol* **5**: 126–140.

Xia, Y., Kong, Y., Thomsen, T.R., and Nielsen, P.H. (2008) Identification and ecophysiological characterization of epiphytic protein-hydrolyzing *Saprospiraceae* ("*Candidatus* Epiflobacter" spp.) in activated sludge. *Appl Environ Microbiol* **74**: 2229–2238.

Yoon, J., Jang, J.-H., and Kasai, H. (2014) *Algisphaera agarilytica* gen. nov., sp. nov., a novel representative of the class *Phycisphaerae* within the phylum *Planctomycetes* isolated from a marine alga. *Antonie Van Leeuwenhoek* **105**: 317–324.

Supporting Information

Additional Supporting Information may be found in the online version of this article at the publisher's web-site:

Appendix S1. Supporting Information Figures.